resonance energy between **1** and **2**. Thus, thermochemically, substitution of hydrogen by fluorine has caused a very small change in the resonance energy of the cyclopropenone.

Conclusions. To obtain a measure of the aromaticity in **2** relative to that in **1**, the properties of the two compounds were compared using several different criteria. These included NMR spectra, geometry, electron distribution, and thermodynamic stability. Compared with appropriate model compounds, the NMR spectra of **2** were very similar to those of **1**. Analysis of the HF/6-31G* wave functions of **1** and **2** revealed that the π-electron distributions, covalent bond orders, and resonance energies were extremely similar for the two compounds. These three criteria suggest that there is a similar degree of aromaticity associated with **1** and **2**. Although the experimental ring geometries of **1** and **2** differed somewhat, the data were not sufficiently compelling to distinguish any aromaticity difference. In this regard, it is important to note that the fluorine atoms influence strongly the σ-electron system of the ring, masking to a large extent any small changes in π delocalization that might occur. Thus, it is clear that small bond length changes may not be useful guides for distinguishing minor changes in aromaticity.

Acknowledgment. This research was supported by NSF Grant CHE-8822674 at the University of Pennsylvania. Acknowledgment is made to the donors of the Petroleum Research Fund, administered by the American Chemical Society, for partial support of the research at The University of Kansas. W.P.D. thanks the Alfred P. Sloan Foundation for a research fellowship.

NMR Detection of *N*-Acyliminium Ion Intermediates Generated from α-Alkoxycarbamates

Yoshinori Yamamoto,* Tomohisa Nakada, and Hisao Nemoto

Contribution from the Department of Chemistry, Faculty of Science, Tohoku University, Sendai 980, Japan. *Received March 11, 1991*

Abstract: The *N*-acyliminium ion intermediates generated from α-alkoxycarbamates in the presence of Lewis acids were for the first time detected by ^1H and ^{13}C NMR. It was confirmed that there is an equilibrium between the starting carbamate and the intermediate and that the equilibrium is highly dependent upon a Lewis acid. By using the saturation transfer method, the rate constant for the formation of the intermediate was obtained. NOE experiments revealed that ((4-methylphenyl)-methylene)methyl(methoxycarbonyl)ammonium methyltrifluoroborate **6** has *E*-geometry.

N-Acyliminium ions **1** are becoming important intermediates in synthetic organic chemistry.[1] The imino carbon atom in **1** is more electron-deficient than the carbon in the Mannich reagent **2**, and thus the amidoalkylating reagent **1** has been frequently used in modern organic synthesis.[2] There are several major

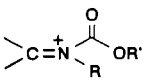

1

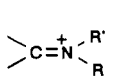

2

synthetic ways to **1**: (i) acylation of imines, (ii) N-protonation of *N*-acylimines, (iii) electrophilic addition to enamides or to *N*-acylimines, (iv) oxidation of amides (removal of a hydride from the α-carbon of amides), and (v) heterolysis of amides bearing a leaving group X on the α-carbon with respect to nitrogen.[1] Perhaps the most frequently used method for generating **1** is the heterolysis of the α-substituted amides (v). For example, α-alkoxycarbamates **3** have been thought to generate *N*-acyliminium ions **1** upon treatment with Lewis acids, which are in situ trapped with nucleophiles giving the product **4** substituted at the α-position via the S_N1 process. It has been proposed without any experimental evidence that there is an equilibrium between **3** and **1**.

However, unambiguous evidence on the formation of **1** from **3** has not been obtained. All previous mechanistic discussions have been based on the analysis of products **4**. Iminium salts **2** (R,

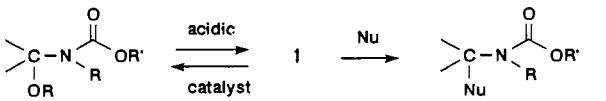

3 4

R′ = H, alkyl, aryl), which are relatively stable, have been detected in solution by NMR,[3] and in some cases the solid structure has been elucidated by X-ray analysis.[3f] The NMR analysis of the adduct between acetyl chloride and benzalaniline revealed that the corresponding α-chloroamide was formed instead of the *N*-acyliminium salt.[4a] Generation of **1** from the N-protonation of *N*-acylimines,[4b,c] from the removal of a hydride from the α-carbon of an amide,[4d] and from the electrophilic addition to *N*-acylimines[4e,f] has been confirmed by NMR. However, the formation of **1** from α-alkoxycarbamates which are synthetically most important has not been verified. We provide for the first time unambiguous evidence that (i) treatment of **3** with certain Lewis acids produces **1**, (ii) there is an equilibrium between **3** and **1**, and (iii) the equilibrium depends upon the Lewis acid used. We

(1) Reviews: (a) Speckamp, W. N.; Hiemstra, H. *Tetrahedron* **1985**, *41*, 4367. (b) Shono, T. *Tetrahedron* **1984**, *40*, 811. (c) Zaugg, H. E. *Synthesis* **1984**, 85 and 181.

(2) Intramolecular reactions, for example: (a) Reference 1. (b) Keck, G. E.; Cressman, E. N. K.; Enholm, E. J. *J. Org. Chem.* **1989**, *54*, 4345. (c) Melching, K. H.; Hiemstra, H.; Klaver, W. J.; Speckamp, W. N. *Tetrahedron Lett.* **1986**, *27*, 4799. Intermolecular reactions: (d) Yamamoto, Y.; Schmid, M. *J. Chem. Soc., Chem. Commun.* **1989**, 1310. (e) Yamada, J.; Sato, H.; Yamamoto, Y. *Tetrahedron Lett.* **1989**, *30*, 5611.

(3) (a) Leonard, N. J.; Paukstelis, J. V. *J. Org. Chem.* **1963**, *28*, 3021. (b) Reinecke, M. G.; Kray, L. R. *J. Org. Chem.* **1966**, *31*, 4215. (c) Olah, G. A.; Kreienbuhl, P. *J. Am. Chem. Soc.* **1967**, *89*, 4756. (d) Pankratz, M.; Childs, R. F. *J. Org. Chem.* **1985**, *50*, 4553. (e) Childs, R. F.; Shaw, G. S.; Lock, C. J. L. *J. Am. Chem. Soc.* **1989**, *111*, 5424. (f) Sorgi, K. L.; Maryanoff, C. A.; McComsey, D. F.; Graden, D. W.; Maryanoff, B. E. *J. Am. Chem. Soc.* **1990**, *112*, 3567. (g) Parkkinen, A.; Mattinen, J.; Lonnberg, H.; Pihlaja, K. *J. Chem. Soc., Perkin Trans. II* **1988**, 827.

(4) (a) Bose, A. K.; Spiegelman, G.; Manhas, M. S. *Tetrahedron Lett.* **1971**, 3167. (b) Uray, G.; Ziegler, E. *Z. Naturforsch.* **1975**, *308*, 245. (c) Krow, G. R.; Pyun, C.; Leitz, C.; Marakowski, J. *J. Org. Chem.* **1974**, *39*, 2449. (d) Cohen, T.; Lipowitz, J. *J. Am. Chem. Soc.* **1964**, *86*, 2514. (e) Würthwein, E. U.; Kupfer, R.; Kaliba, C. *Angew. Chem., Int. Ed. Engl.* **1983**, *22*, 252. (f) Krestel, M.; Kupfer, R.; Allmann, R.; Würthwein, E. U. *Chem. Ber.* **1987**, *120*, 1271.

0002-7863/92/1514-121$03.00/0 © 1992 American Chemical Society

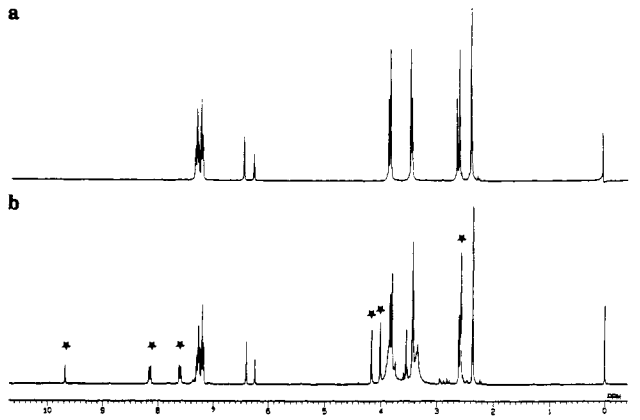

Figure 1. (a) ^1H NMR of **5a** and (b) ^1H NMR of **5a** + BF_3.

Table I. Effect of BF_3·OMe_2 upon the Ratio of **6a**/**5a**

BF_3·OMe_2 (equiv)	ratio of **6a**:**5a**	BF_3·OMe_2 (equiv)	ratio of **6a**:**5a**
0	0:100	3	50:50
1	22:88	4	56:44
2	40:60	5	64:36

also report the determination of geometry of **1**.

Results and Discussion

^1H NMR Spectra. We chose **5a** as a starting material, because of the simplicity of its spectra. Initially we used **5b** for the mechanistic study, since its intermolecular reaction with allylic tins in the presence of Lewis acids produced the corresponding imine–allyl condensation product with an interesting diastereoselectivity.[2d] However, the spectra of two ethoxy protons and aromatic protons appeared as multiplets and those analyses were not straightforward. Treatment of **5a** with 1 equiv of BF_3·OMe_2 in $CDCl_3$ at −55 °C produced the spectra shown in Figure 1 (eq 1). The spectra of **5a** is shown in Figure 1a. The tolyl methyl proton appeared at δ 2.35 ppm (in $CDCl_3$) as a singlet, but other methyl protons were observed as two singlet peaks owing to the presence of two rotational isomers: NMe, δ 2.61 and 2.56 ppm; OMe, δ 3.44 and 3.41 ppm; CO_2Me, δ 3.83 and 3.81 ppm. The H^b proton also appeared as two singlets at δ 6.42 and 6.24 ppm (Figure 1a). The new peaks shown by stars appeared after treatment with BF_3·OMe_2 (Figure 1b). The singlet at δ 9.68 ppm corresponded to the methine proton H^a. The aromatic protons shifted to δ 8.15 (d, J = 8 Hz) and δ 7.60 (d, J = 8 Hz) ppm owing to the neighboring plus charge. Two methyl protons appeared at δ 4.17 (OCH_3) and δ 4.01 ppm (NCH_3). The methyl protons of the tolyl group appeared at 2.57. The broad singlet at δ 3.34 ppm corresponded to free Me_2O. It is suggested that the broad singlet at δ 3.85 ppm and the singlet at δ 3.55 ppm correspond to Me_2O·BF_3 and (MeO)·BF_3, respectively. The ratio of **6** to **5a** was obtained from the area ratio of H^a to H^b. The effect of the amount of BF_3·OMe_2 upon the ratio of **6a** to **5a** was investigated at −55 °C. As shown in Table I, the ratio increased with an increase of each equivalent of BF_3·OMe_2. A plot of the ratio vs 0–5 equiv of BF_3·OMe_2 gave a straight line (Figure 2), indicating the presence of an equilibrium between **6a** and **5a**.

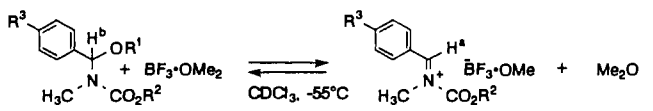

6

5a : $R^1 = R^2 = R^3 = CH_3$
b : $R^1 = R^2 = Et$, $R^3 = H$
c : $R^1 = CD_3$, $R^2 = CH_3$, $R^3 = CH_3$ (1)
d : $R^1 = R^2 = CH_3$, $R^3 = NO_2$
e : $R^1 = R^2 = CH_3$, $R^3 = H$
f : $R^1 = R^2 = CH_3$, $R^3 = OCH_3$
g : $R^1 = R^3 = CH_3$, R^2 = menthyl
h : $R^1 = R^3 = CH_3$, R^2 = 8-phenylmenthyl

Table II. Chemical Shifts of the C_1 and H_1 of Imine Derivative[a]

compounds	X: OMe	X: Me	X: H
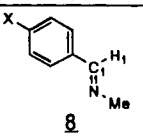 **8**	C_1 161.7 161.4 H_1 8.21	162.3 8.22	162.4 8.29
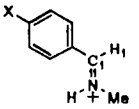 **9**			8.70[b]
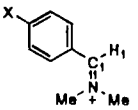 **10**		171.3 (DMSO-d_6) 9.18 (DMSO-d_6)	
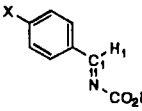 **11**			170.5[c] (177.2[e]) 9.00[c] (9.54[d,e])
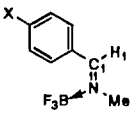 **12**		171.9 171.3 8.69	172.2 8.77
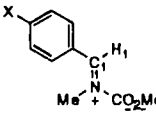 **13**	171.0 170.4 9.53	174.8 9.68 9.77–9.83[f]	176.9 9.85
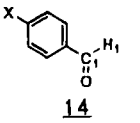 **14**	190.7 9.89	191.9 9.95	192.4 10.05

[a] In $CDCl_3$, −55 °C or room temperature, Lewis acid, BF_3·OMe_2; internal standard, TMS. [b] In SO_2, −60 °C, ref 3c. [c] Kupfer, P.; Meier, S.; Würthwein, E.-U. *Synthesis* **1984**, 688. [d] Protonated form: ref 4c. [e] Protonated form: ref 4f. [f] Lewis acid: TMSOTf or Tf_2O.

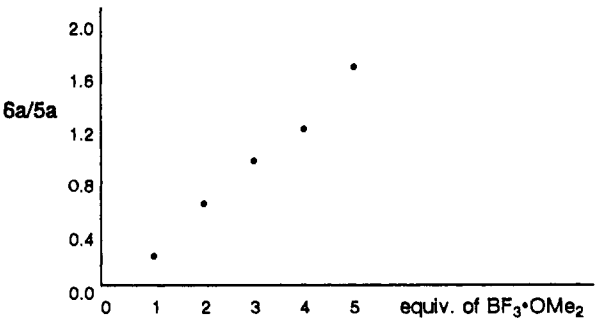

Figure 2. A plot of the ratio of **6a**/**5a** vs 0–5 equiv of BF_3·OMe_2.

Instead of BF_3·OMe_2, TMSOTf was used to clarify the peaks due to free OMe_2 and BF_3·OMe_2. Similarly, the spectra of the acyliminium ion were obtained along with those of **5a** (Figure 3a, see supplementary material). From these spectra, it is clear that the assignment mentioned above on Me_2O·BF_3, (MeO)·BF_3, and Me_2O is correct. Further, we prepared the deuterated α-methoxycarbamate **5c** and obtained the spectra (Figure 3b, see supplementary material) upon treatment with TMSOTf. It was confirmed that the signals at δ 3.41 and 3.44 ppm in Figure 1a were due to the α-methoxy group.

The use of either BF_3·OMe_2 or TMSOTf produced a mixture of the acyliminium ion and the starting material (**5a** or **c**). In-

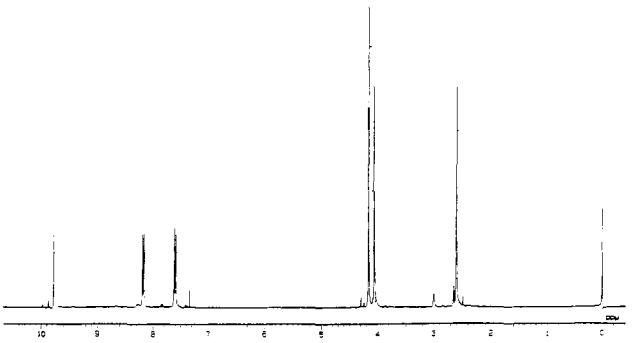

Figure 4. ^1H NMR of **5c** + Tf_2O.

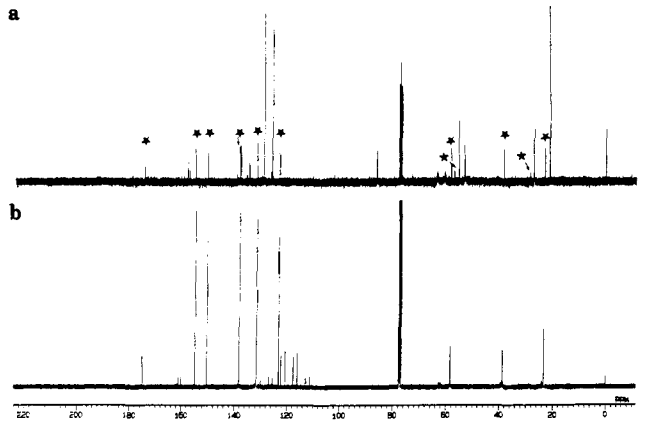

Figure 5. (a) ^{13}C NMR of **5a** + BF_3 and (b) ^{13}C NMR of **5c** + Tf_2O.

terestingly, however, treatment of **5c** with 1 equiv of $(CF_3SO_2)_2O$ afforded the iminium ion exclusively (Figure 4). A very clean spectrum of the acyliminium ion was obtained! Presumably, $CF_3SO_2OCD_3$ would be stable enough and cleavage into $CF_3SO_2^+$ and $^-OCD_3$ must be difficult under the reaction conditions (eq 2). Therefore, the equilibrium is shifted largely to the right. On the other hand, there may be an exchange between $^-BF_3(OMe)$ and Me_2O in eq 1 or between OSO_2CF_3 and $(CH_3)_3SiOCD_3$ in the case of TMSOTf.

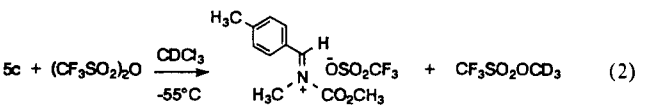

(2)

^{13}C NMR Spectra. The ^{13}C NMR spectra of the *N*-acyliminium ions, obtained from **5a** in the presence of BF_3·OMe_2 and from **5c** in the presence of $(CF_3SO_2)_2O$, are shown in Figure 5. The new peaks appeared by treatment with BF_3·OMe_2 are indicated by stars. The methylene carbon of **6a** appeared at δ 174.8, suggesting the presence of a strong positive charge at the carbon. The peaks indicated by arrows at around 28 and 56 ppm in Figure 5a presumably correspond to Me_2O, Me_2O·BF_3, or MeO·$^-BF_3$, but the precise assignment was not performed.

NOE Experiments and Saturation Transfer. To our surprise the irradiation of the H^a proton of **6a** in eq 1 caused the partial disappearance of the H^b proton of **5a** (Figure 6a). The H^b proton almost completely disappeared upon irradiation of the H^a proton of the acyliminium ion generated by TMSOTf (Figure 6b). These observations clearly indicated that there is an equilibrium between **5a** and **6a**, and the rate constant k^+ in the presence of TMSOTf is much larger than that in the presence of BF_3·OMe_2. When the exchange rate in a chemical system (A and B) (eq 3) is slow in comparison with the time scale of NMR, the saturation of a certain nucleus in B by irradiation leads to a partial or complete saturation of the corresponding nucleus in A if the shift from B to A takes place before complete relaxation of the irradiated nucleus (saturation transfer).[5] The relation between the signal intensity (I_A) before irradiation and that of the nucleus A ($I_{A'}$) during irradiation

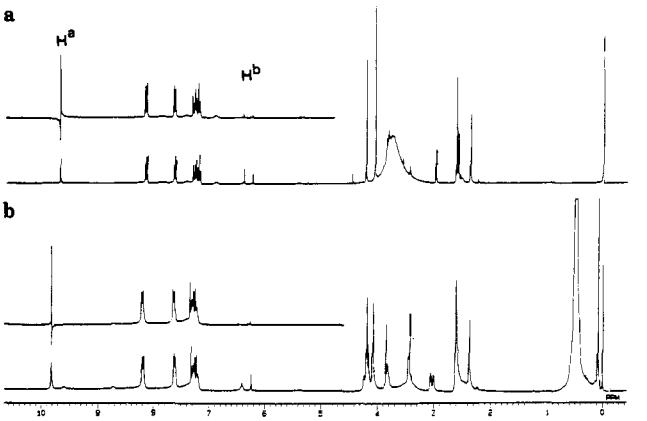

Figure 6. (a) Decoupling of **5a** + BF_3 and (b) decoupling of **5a** + TMSOTf.

of the nucleus B is expressed as follows (eq 4).[5] By using eq 5, the rate constant k^+ in eq 3 can be obtained.

$$\mathbf{5a} \underset{k^-}{\overset{k^+}{\rightleftharpoons}} \mathbf{6a} \qquad A \underset{k_{BA}}{\overset{k_{AB}}{\rightleftharpoons}} B \tag{3}$$

$$I'_A = \frac{\tau_A}{\tau_A - T_{1A}} I_A \tag{4}$$

T_{1A}: the relaxation time of nucleus A

τ_A: the lifetime of A

then

$$k_{AB} = \frac{1 - (I'_A/I_A)}{T_{1A}}; \; T'_{1A} = T_{1A}(I_{A'}/I_A) \tag{5}$$

The saturation transfer method in the BF_3·OMe_2 mediated system at −52 °C gave $T_{1A'} = 1.24$ s and $I_{A'}/I_A = 0.896$, in which A and A' corresponded to the nucleus H^b of **5a**. T_{1A} was obtained from a separate experiment. Accordingly, $k^+ = 0.084$ s^{-1} and $\tau_A = 1/k^+ = 12$ s. If the rate is first-order relative to the substrate, $rate_A = k^+[A] = 0.084 \times 0.13 = 0.011$ mol L^{-1} s^{-1}. The data at −31 °C were obtained in a similar way: $k^+ > 9.1$ s^{-1}. The exchange speed was enhanced more than 10 times with a 20 °C rise in temperature. As mentioned above, the irradiation in the presence of TMSOTf caused almost complete disappearance of the H^b proton even at −55 °C. As a result the exchange rate was too rapid ($I_{A'}/I_A \sim 0$) to permit k^+ to be obtained.

The Geometry of 6. The differential NOE spectra of **6a** was obtained at −55 °C in $CDCl_3$. When H^a was irradiated, NOEs were observed at the ortho protons of the aromatic ring. Both H^a and the methyl protons of NMe exhibited NOEs upon irradiation of the ortho protons. No NOE was observed between H^a and the NMe. Accordingly it is clear that **6a** has adopted *E* geometry.

Other Observations. Detection of the acyliminium ion from **5d** was tried by using BF_3·OMe_2, TMSOTf, and Tf_2O. However, such a species could not be detected in $CDCl_3$ at −55 °C. The iminium ion derived from **5e** was detected at −55 °C with the aid of Tf_2O, and the ratio of the iminium ion to **5e** was 1:4. Under the same conditions, **5a** gave the ratio of 100:0. Treatment of **5f** with 1 equiv of BF_3·OMe_2 produced the ratio of 1:3. Accordingly, it is clear that electron-donating groups such as Me and OMe stabilize the intermediate, while electron-withdrawing groups such as NO_2 destabilize the iminium ion. Normally, **6a** was produced in $CDCl_3$. Formation of **6a** in CD_2Cl_2 was much faster than its formation in $CDCl_3$, indicating that the equilibrium was affected by the solvent.

In order to extend the present findings to the molecular design of asymmetric synthesis, we next investigated the system having a chiral auxiliary at the ester group R^2. Treatment of the menthyl

(5) Sandström, J. *Dynamic NMR Spectroscopy*; Academic Press: New York, 1982.

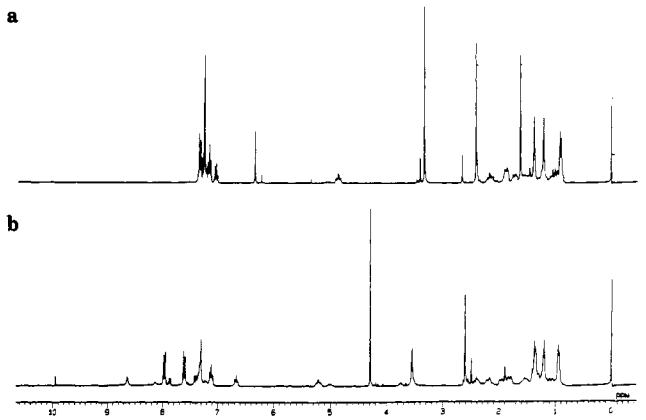

Figure 8. (a) ^1H NMR of **5h** and (b) ^1H NMR of **5h** + Tf_2O.

derivative **5g** with BF_3·OMe_2 in $CDCl_3$ gave the corresponding acyliminium ion (Figure 7, see supplementary material). The H^a proton of **5g** appeared at δ 6.455, 6.447, 6.33, and 6.30 ppm. Since **5g** consists of two diastereomers and each isomer has two rotational isomers, **5g** actually consists of four stereoisomers. The H^b proton of **6g** appeared at δ 9.68 ppm, and a small peak at about 10 ppm corresponded to the aldehyde proton of tolylaldehyde which was formed by partial hydrolysis of **5g**. Formation of the aldehyde was often observed upon the addition of a Lewis acid (for example, Figures 1b, 4b, and 8b). The NMe protons of **5g** were observed at δ 2.61, 2.57, and 2.56 ppm. Accordingly, the chemical shifts of representative protons of **5g** and **6g** are nearly the same as those of **5a–c** and **6a–c**.

The ^1H NMR spectra of **5h** and **6h** are shown in Figure 8 (parts a and b, respectively). Two diastereoisomers of **5h** were separated by HPLC, and each isomer was treated independently with Tf_2O. It was confirmed that each isomer gave the same NMR spectrum upon treatment with the Lewis acid. In Figure 8a, only one of the two diastereomers is shown. The H^a proton of **5h** appeared at δ 6.33 and 6.21 ppm. These chemical shifts are somewhat shielded in comparison with those of **5g**. NMe protons were observed at δ 1.62 (major) and 2.66 (minor) ppm, indicating that the protons of a major isomer of two rotamers were highly shielded. Very interestingly, the H^b proton of **6h** was observed at δ 8.64 ppm, and the methyl protons of NMe of **6h** appeared at δ 3.54 ppm. The H^b proton and NMe protons of ordinary acyliminium ions such as **5a–g** appeared at ca. δ 9.6–9.9 and 4.0 ppm, respectively. Accordingly, it is clear that the H^b and NMe protons are shielded by the aromatic ring of the 8-phenylmenthyl group. The ortho protons (δ 7.61 ppm) of the tolyl group of **6h** were also shielded, but the meta protons (δ 7.97 ppm) and the methyl protons (δ 2.61 ppm) were not. Taken together, **6h** adopts the configuration of either **7a** (cisoid) or **7b** (transoid). It is not so easy at the present moment to establish which geometry is preferable. However, the following observations suggest that **7b** is much more stabilized in comparison with **7a**: (1) the para proton (δ 6.60 ppm) of the 8-phenylmethyl group is highly shielded by the tolyl group; (2) only the ortho protons of the tolyl group are shielded; (3) a molecular model of **7b** agrees with the above observations. We are now investigating an asymmetric induction via **7**, and the result will tell us which geometry is involved in a nucleophilic addition.

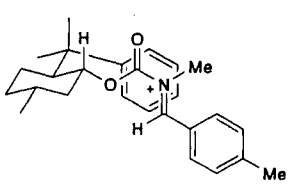

7b (transoid)

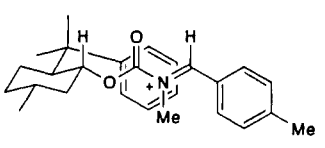

7a (cisoid)

Conclusion. The ^1H and ^{13}C chemical shifts of imine proton H_1 and carbon C_1 of the representative imines, their BF_3 complexes, and iminium ions are summarized in Table II. It is well accepted that the difference in the chemical shifts of two different molecules is primarily a reflection of the electron density difference, if the hybridization and stereochemistry of the corresponding atom are nearly identical. When X is Me, the following order of δ^+ at the C_1 atom is observed: the acyliminium ion **13** > alkyliminium ion **10** > imine–BF_3 complex **12** > imine **8**. When X is H, the order is **13** > **12** > the acylimine > the iminium ion **9** > **8**. Consequently, it is clear that the acyliminium ion **13** is the most electrophilic species among the imine intermediates (**8–13**). However, even **13** is less electrophilic in comparison with the corresponding aldehyde **14**. The activation of imines has been carried out mostly by the coordination of Lewis acids to the nitrogen atom. The present findings clearly indicate that an acyliminium ion is a much more strongly activated form of the C=N double bond than an imine–Lewis acid complex.

Experimental Section

^1H and ^{13}C NMR spectra were recorded on a JEOL GSX-270 NMR at 270 and 67.5 MHz, respectively, in $CDCl_3$, and the chemical shifts were indicated in ppm with δ values relative to internal TMS at 24 °C unless otherwise noted. IR spectra were taken with a HITACHI 260-10 spectrometer. High-resolution mass spectra (EI) were measured with a JEOL JMS-HX110 spectrometer. Elemental analyses were performed at the analytical center of Tohoku University. $CDCl_3$, BF_3·OMe_2, TMSOTf, and Tf_2O were purchased from Aldrich and used as such.

Synthesis of α-Alkoxycarbamates. Synthesis of **5c** is representative. In a 30-mL flask under Ar were placed *N*-(*p*-methylbenzylidene)-methylamine (1.34 g, 10.1 mmol) and 10 mL of CH_2Cl_2. The flask was cooled to 0 °C, and ethyl chloroformate (1.20 mL, 12.6 mmol) was added. The flask was warmed slowly to room temperature, stirred for 1 h, and then cooled again to 0 °C. Triethylamine (1.7 mL, 12.1 mmol) and CD_3OD (0.5 mL, 12.3 mmol) were added, and the resulting mixture was stirred overnight at room temperature. The solvent was removed under reduced pressure, and hexane was added. The precipitate was separated using a centrifuge. The organic layer was separated and condensed giving yellow oil (2.15 g). Purification by flash silica gel column chromatography (Merck) using hexane–EtOAc 20:1 as an eluant gave a colorless oil (1.92 g, 79%). The same procedure was used for the synthesis of **5a–f**.

***N*-(Methoxycarbonyl)-*N*-methyl-1-methoxy-*p*-methylbenzylamine (5a)**: colorless oil; ^1H NMR ($CDCl_3$) δ 2.32 (s, 3 H), 2.55 and 2.59 (s, 3 H), 3.41 (s, 3 H), 3.78 and 3.80 (s, 3 H), 6.20 and 6.40 (s, 1 H), 7.14 (d, J = 8 Hz, 2 H), 7.25 (m, 2 H); ^{13}C NMR ($CDCl_3$) δ 21.12, 27.02, 52.76 and 52.83, 55.18 and 55.35, 86.56 and 86.64, 126.11, 128.96, 135.23, 137.66; IR (CCl_4) 2960, 1715, 1455, 1395, 1333, 1158, 1095 cm^{-1}. Anal. Calcd for $C_{12}H_{17}NO_3$: C, 64.55; H, 7.67; N, 6.27. Found for C, 64.37; H, 7.90; N, 6.57.

***N*-(Ethoxycarbonyl)-*N*-methyl-1-ethoxybenzylamine (5b)**: colorless oil; ^1H NMR ($CDCl_3$) δ 1.21–1.34 (m, 6 H), 2.57 and 2.59 (s, 3 H), 3.54–3.70 (m, 2 H), 4.15–4.35 (m, 3 H), 6.38 and 6.53 (s, 1 H), 7.28–7.39 (m, 5 H); ^{13}C NMR ($CDCl_3$) δ 13.92, 14.67 and 14.97, 27.17, 61.53 and 61.57, 62.94 and 63.21, 84.75 and 84.81, 126.21 and 126.30, 127.87 and 127.94, 128.22, 138.59, 157.46; IR (CCl_4) 2980, 1710, 1445, 1395, 1320, 1150, 1090 cm^{-1}; HRMS calcd for $C_{13}H_{19}NO_3$ m/z 237.1365, found for m/z 237.1367. Anal. Calcd for $C_{13}H_{19}NO_3$: C, 65.80; H, 8.07; N, 5.90. Found for C, 65.69; H, 8.24; N, 5.88.

***N*-(Methoxycarbonyl)-*N*-methyl-1-trideuteriomethoxy-*p*-methylbenzylamine (5c)**: colorless oil; ^1H NMR ($CDCl_3$) δ 2.35 (s, 3 H), 2.55 and 2.58 (s, 3 H), 3.78 (s, 3 H), 6.20 and 6.39 (s, 1 H), 7.14 (d, J = 8 Hz, 2 H), 7.20–7.28 (m, 2 H); ^{13}C NMR ($CDCl_3$) δ 21.12, 27.03, 52.78, 86.54, 126.10, 128.97, 135.24, 137.69; IR (CCl_4) 2960, 1705, 1455, 1395, 1325, 1160, 1115, 1095 cm^{-1}; HRMS calcd for $C_{12}H_{14}D_3NO_3$ m/z 226.1397, found for m/z 226.1396.

***N*-(Methoxycarbonyl)-*N*-methyl-1-methoxy-*p*-nitrobenzylamine (5d)**: yellow crystal; ^1H NMR ($CDCl_3$) δ 2.55 and 2.58 (s, 3 H), 3.46 (s, 3 H), 3.83 and 3.86 (s, 3 H), 6.30 and 6.49 (s, 1 H), 7.58 (d, J = 8 Hz, 2 H), 8.21 (d, J = 8 Hz, 2 H); ^{13}C NMR ($CDCl_3$, internal standard: $CDCl_3$) δ 27.02, 53.07, 55.50, 85.55, 123.49, 127.27, 145.33, 147.74; IR (KBr) 2970, 1720, 1525, 1455, 1350, 1330, 1150, 1090 cm^{-1}; HRMS calcd for $C_{11}H_{14}N_2O_5$ m/z 254.0903, found for m/z 254.0903.

N-(Methoxycarbonyl)-*N*-methyl-1-methoxybenzylamine (5e): colorless oil; ^{1}H NMR ($CDCl_3$) δ 2.56 and 2.59 (s, 3 H), 3.43 (s, 3 H), 3.80 and 3.82 (s, 3 H), 6.24 and 6.43 (s, 1 H), 7.27-7.39 (m, 5 H); ^{13}C NMR ($CDCl_3$, at -55 °C) δ 27.15 and 27.23, 53.03 and 53.27, 55.22 and 55.31, 85.90 and 86.07, 125.82 and 125.91, 127.98 and 128.07, 128.26 and 128.29, 128.66 and 128.99, 137.42 and 137.57, 157.14 and 157.87; IR (CCl_4) 2950, 1715, 1455, 1395, 1330, 1155, 1100, 990 cm^{-1}; HRMS calcd for $C_{11}H_{15}NO_3$ m/z 209.1052, found for m/z 209.1049.

N-(Methoxycarbonyl)-*N*-methyl-1-methoxy-*p*-methoxybenzylamine (5f): colorless oil; ^{1}H NMR ($CDCl_3$) δ 2.55 and 2.58 (s, 3 H), 3.40 (s, 3 H), 3.80 (s, 6 H), 6.18 and 6.36 (s, 1 H), 6.87 (d, J = 8 Hz, 2 H), 7.23-7.32 (m, 2 H); ^{13}C NMR ($CDCl_3$) δ 26.95, 52.78, 55.25 and 55.35, 86.39, 113.62, 127.37, 130.30, 159.34; IR (CCl_4) 2995, 2950, 2830, 1705, 1615, 1510, 1450, 1325, 1250, 1175, 1150, 1090, 1040, 985 cm^{-1}; HRMS calcd for $C_{12}H_{17}NO_3$ m/z 239.1158, found for m/z 239.1161.

Synthesis of Chiral α-Alkoxycarbamates. Synthesis of **5h** is representative. In a 200-mL flask under Ar were placed 8-phenylmenthol (5.59 g, 24.0 mmol), benzene (150 mL), and trichloromethyl chloroformate (TCF) (6.0 mL, 50 mmol). The mixture was refluxed at 100 °C for 13 h and then stirred at room temperature for 18 h. Pyridine (2.2 mL, 27.2 mmol) was added. Complete consumption of the starting materials was confirmed by TLC analysis. The solvent was removed under reduced pressure, and then benzene was added. The mixture was filtered through Celite under reduced pressure. Removal of solvent gave crude 8-phenylmenthyl chloroformate, which was immediately transferred to a 200-mL flask under Ar and dissolved in 60 mL of CH_2Cl_2. A CH_2Cl_2 (10 mL) solution of *N*-(*p*-methylbenzylidene)methylamine (3.21 g, 24.1 mmol) was prepared in a 50-mL flask under Ar, and the solution was transferred to the 200-mL flask cooled to 0 °C through a double-ended needle. Stirring was continued for 3 h at room temperature, and the flask was cooled to 0 °C. Triethylamine (4.0 mL, 28.7 mmol) and then methanol (2.0 mL, 49.4 mmol) were added. Stirring was continued overnight at room temperature. A similar isolation procedure as mentioned above was used. Crude yellow oil (9.59 g) was obtained. Purification with a flash silica gel column chromatography using hexane-EtOAc (30:1) as an eluant gave a colorless oil (5.53 g, 54%).

N-[(-)-Menthoxycarbonyl]-*N*-methyl-1-methoxy-*p*-methylbenzylamine (5g): colorless oil; ^{1}H NMR ($CDCl_3$, at -55 °C) δ 0.7-2.3 (m, 15 H), 0.93 (br s, 3 H), 2.37 (s, 3 H), 2.56 and 2.57 and 2.61 (s, 3 H), 3.42 and 3.44 (s, 3 H), 4.70-4.90 (m, 1 H), 6.30 and 6.33 and 6.45 and 6.46 (s, 1 H), 7.19-7.32 (m, 4 H); ^{13}C NMR ($CDCl_3$) δ 16.21, 16.61, 20.78, 21.07, 22.04, 23.30, 23.80, 26.65, 26.97, 31.45, 34.38, 41.57, 47.49, 55.04, 75.51, 86.39, 126.02, 128.92, 130.09, 135.40, 137.52; IR (CCl_4) 2970, 2940, 2880, 1700, 1445, 1400, 1330, 1310, 1165, 1150, 1090, 980 cm^{-1}; HRMS calcd for $C_{21}H_{33}NO_3$ m/z 347.2461, found for m/z 347.2465.

N-[(-)-(8-Phenylmenthoxy)carbonyl]-*N*-methyl-1-methoxy-*p*-methylbenzylamine (major isomer) (5h): colorless oil; ^{1}H NMR ($CDCl_3$) δ 0.85-2.15 (m, 8 H), 0.89 (d, J = 7 Hz, 3 H), 1.23 (s, 3 H), 1.35 (s, 3 H), 1.88 and 2.62 (s, 3 H), 2.37 (s, 3 H), 3.33 (s, 3 H), 4.86 (dt, J = 4 Hz, J = 10 Hz, 1 H), 6.10 and 6.33 (s, 1 H), 6.99 (m, 1 H), 7.09-7.28 (m, 8 H); ^{13}C NMR ($CDCl_3$) δ 21.16, 21.83, 24.82, 26.21, 26.69, 28.29, 31.35, 34.67, 39.65, 42.41, 50.55, 55.19, 75.32, 86.23, 124.87, 125.19, 126.22, 127.93, 128.76, 135.30, 137.48, 152.22, 156.55; IR (CCl_4) 2960, 2930, 1695, 1445, 1395, 1320, 1155, 1090, 980 cm^{-1}. Anal. Calcd for $C_{27}H_{37}NO_3$: C, 76.56; H, 8.80; N, 3.31. Found for C, 76.42; H, 8.93; N, 3.33.

N-[(-)-(8-Phenylmenthoxy)carbonyl]-*N*-methyl-1-methoxy-*p*-methylbenzylamine (minor isomer) (5h): colorless oil; ^{1}H NMR ($CDCl_3$) δ 0.86-2.10 (m, 8 H), 0.89 (d, J = 6 Hz, 3 H), 1.24 (s, 3 H), 1.38 (s, 3 H), 1.93 and 2.58 (s, 3 H), 2.30 and 2.32 (s, 3 H), 3.36 and 3.40 (s, 3 H), 4.87 (dt, J = 4 Hz, J = 10 Hz, 1 H), 5.91 and 6.34 (s, 1 H), 7.09-7.33 (m, 9 H).

NMR Measurement. The α-alkoxycarbamates **5** (0.5 ~ 0.1 mmol) were placed in a 5-mm NMR tube with a septum cap under Ar atmosphere. $CDCl_3$ (0.65 mL) and 0.05 mL of $CDCl_3$ containing 1% TMS were added. The solvent was dried with molecular sieves (4A) prior to use. The tube was cooled to an appropriate temperature, and then the Lewis acid was added by a microsyringe. The tube was transferred rapidly to a NMR probe which was cooled to -55 °C.

Supplementary Material Available: ^{1}H NMR spectra of **5a** + TMSOTf and **5c** + TMSOTf (Figure 3a,b) and **5g** and **5g** + BF_3 (Figure 7a,b) (2 pages). Ordering information is given on any current masthead page.

NMR Imaging of Anisotropic Solid-State Chemical Reactions Using Multiple-Pulse Line-Narrowing Techniques and ^{1}H T_1 Weighting

Leslie G. Butler,*,†,1a David G. Cory,‡,1b Kerry M. Dooley,1c Joel B. Miller,1b and Allen N. Garroway*,1b

Contribution from Code 6122, Chemistry Division, Naval Research Laboratory, Washington, D.C. 20375-5000, Department of Chemistry, Louisiana State University, Baton Rouge, Louisiana 70803-1804, and Department of Chemical Engineering, Louisiana State University, Baton Rouge, Louisiana 70803-7303. *Received May 20, 1991*

Abstract: The reactions of substituted benzoic acid crystals and powders with ammonia gas have been monitored using solid-state ^{1}H NMR imaging techniques. The reactions are inherently (crystal) or by design (powder) spatially anisotropic: For a crystal of 4-bromobenzoic acid, the expected reaction anisotropy was not seen, either optically or with ^{1}H NMR imaging, most likely due to poor crystal quality or an unexpected crystal morphology. Nevertheless, some anisotropy in the reaction was observed and the extent of reaction was obtained from the NMR images. For a deep bed of powdered toluic acid, an anisotropic reaction profile is found. The reaction of the more exposed top layers of the bed is rapid whereas there is a delay in the reaction of the bottom layers associated with the rate of diffusion of ammonia into the bed. The apparent reaction rate constant, k = 5 (2) × 10^{-4} mol^{-1} m^3 s^{-1}, and the effective diffusivity, D_e = 1.0 (4) × 10^{-5} m^2 s^{-1}, were obtained from a fit to a simultaneous diffusion with reaction model for a slab. This work is the first application of ^{1}H NMR imaging, using multiple-pulse line-narrowing techniques, for monitoring a chemical reaction. For this work, the special advantage of line narrowing is that the images are weighted not by the ^{1}H T_2 but rather by the T_1 relaxation time. Thus, for the materials studied herein, selection of an appropriate relaxation time in the NMR experiment enables observation of either the reaction product or the total sample.

Introduction

Anisotropic chemical reactions are common. Reactions at interfaces are necessarily anisotropic, for example, the reaction of oxygen with a silicon surface.[2] However, it is difficult to visualize the progress of such anisotropic chemical reactions.

* Author to whom correspondence should be addressed.
† Fellow of the Alfred P. Sloan Foundation (1989-1991).
‡ Present address: Bruker Instruments, Inc., Manning Park, Billerica, MA 01821.

(1) (a) Department of Chemistry, Louisiana State University. (b) Naval Research Laboratory. (c) Department of Chemical Engineering, Louisiana State University.
(2) Deal, B. E. Grove, A. S. *J. Appl. Phys.* **1965**, *36*, 3770-8.

0002-7863/92/1514-125$03.00/0 © 1992 American Chemical Society